Large-scale Structure and Turbulence Transport during Solar Minimum - Comparison of PSP's First Five Orbits with a Global 3D Reynolds-averaged MHD Model

Rohit Chhiber

University of Delaware & NASA Goddard Space Flight Center

Collaborators: William Matthaeus, Arcadi Usmanov, Melvyn Goldstein

WHPI Workshop

13-17 September 2021

Introduction and Motivation

- Solar wind known to be turbulent, with structure and fluctuations across scales
- Turbulent cascade - mechanism for coronal heating, acceleration and heating of solar wind; Fluctuations influence SEP transport
- Not computationally feasible to resolve fluctuations in global models
- Here we use a global MHD model coupled to turbulence transport model; compare an ensemble of runs with data aggregated from five PSP orbits
- In particular, examine long-term radial trends over 2 years during solar min

Global simulation with turbulence modeling – Schematic of Reynolds-Averaging Approach

Reynolds decomposition splits fields (ã) into mean (a) and fluctuation (a'; arbitrary amplitude): $\tilde{\mathbf{a}} = \mathbf{a} + \mathbf{a}'$

Explicitly resolve large-scale/mean flow

Large scale (mean field) model equations:
- Momentum
- Magnetic field
- Density
- internal energies (Te & Tp)

NEW TERMS:
- Fluctuation pressure
- Reynolds stresses
- Turbulent electric field
- Heat function/dissipation

Closures:
- Eddy viscosity (kinetic & magnetic)
- Production/mixing terms
- Turbulent transport coefficients

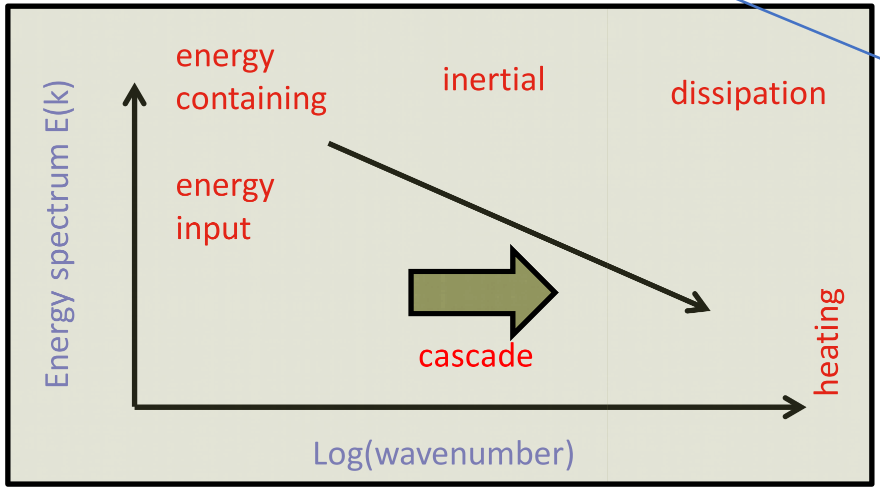

Evaluate required turbulence parameters: Transport equations for energy, cross helicity, correlation scales

Describe fluctuations statistically

Plasma kinetic theory:
- branching between e/p heating

Coupled system - turbulence heats and accelerates wind; gradients in large-scale fields drive turbulence

Turbulence Transport

- Three equations describing statistical properties of turbulence

- $Z^2 = \langle v'^2 + b'^2 \rangle$ is (twice the incompressible yurbulent energy per unit mass
- $\sigma_c = \dfrac{2\langle \mathbf{v}' \cdot \mathbf{b}' \rangle}{\langle v'^2 + b'^2 \rangle}$ is the normalized cross helicity
- λ is the similarity (correlation) length scale

- Physically and empirically motivated ICs and BCs
- Magnetogram-based or dipolar source magnetic field
- Numerical domain from coronal base to few AU
- Model well tested against 1+ AU observations

See Usmanov et al., 2018 for more details

Parker Solar Probe

- We use MAG and SPC measurements from first five orbits to compare observations with bulk-flow and turbulence parameters from model
- Five runs with appropriate magnetogram B.C.s
- r $\sim$28 to 200 $R_\odot$

- Data resampled to 1-sec cadence
- Fluctuations computed using a rolling average over a 2-hour window; e.g.: $\boldsymbol{b} = \boldsymbol{B} - \langle \boldsymbol{B} \rangle$
- Autocorrelations computed using Blackman-Tukey method (Matthaeus et al. 1982) over 1-day intervals. Correlation times then converted to lengths using Taylor hypothesis (e.g., Chen et al. 2020)

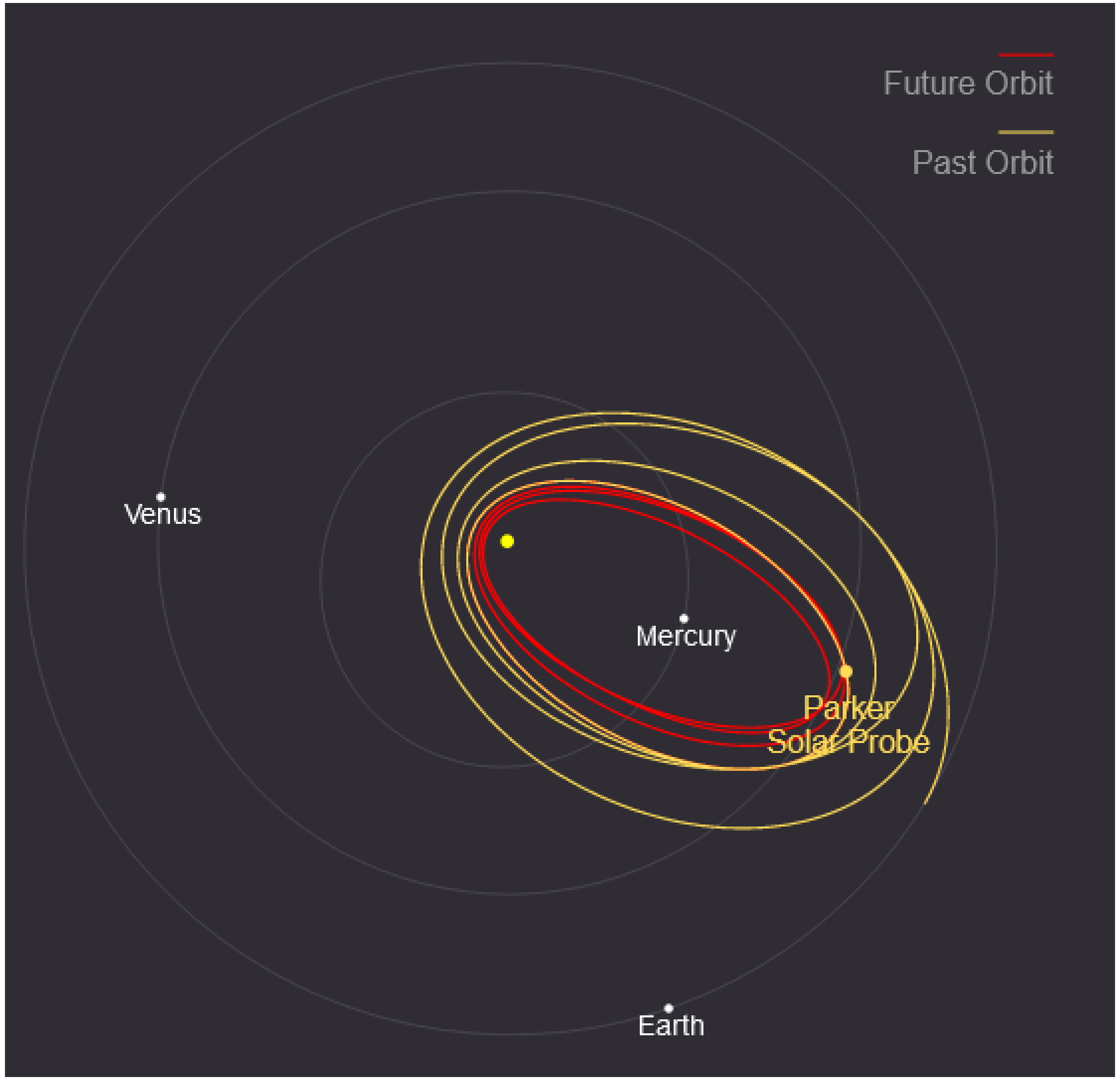

Figure courtesy JHU APL

Comparison of model using April 2019 magnetogram with PSP O2 data

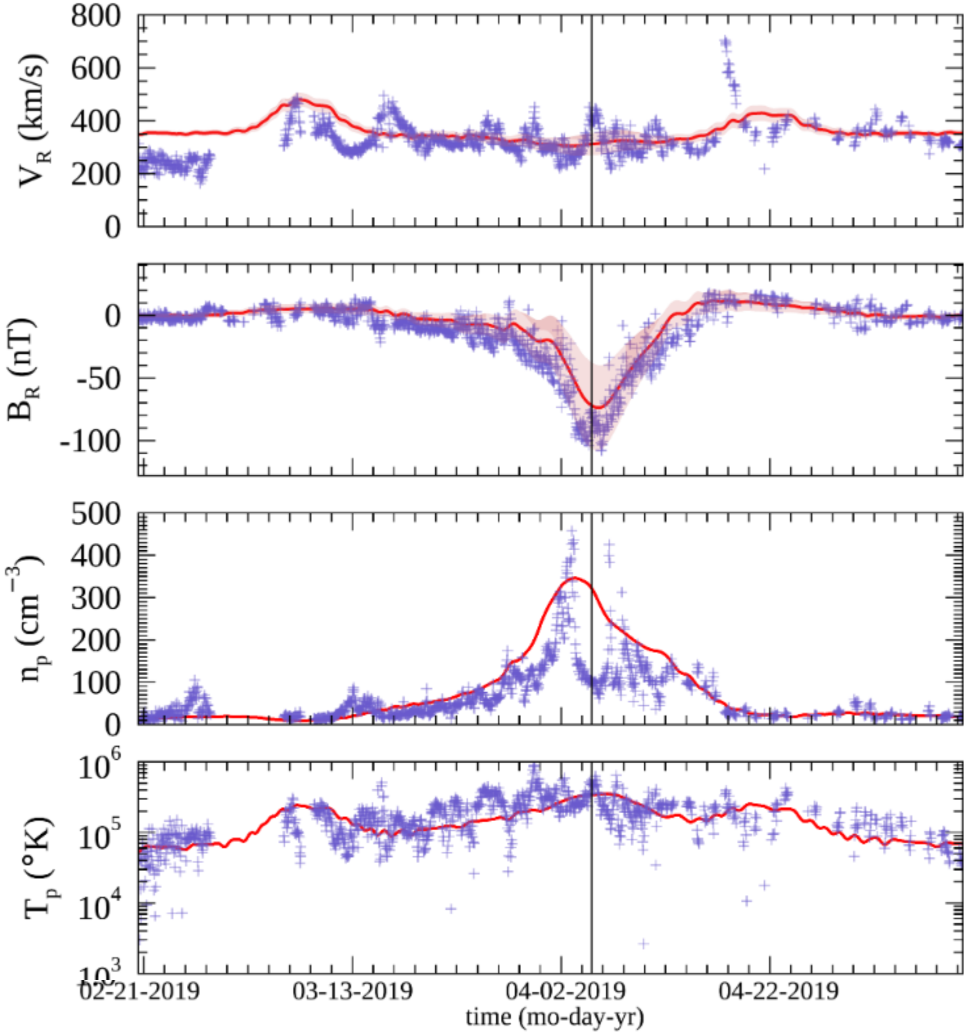

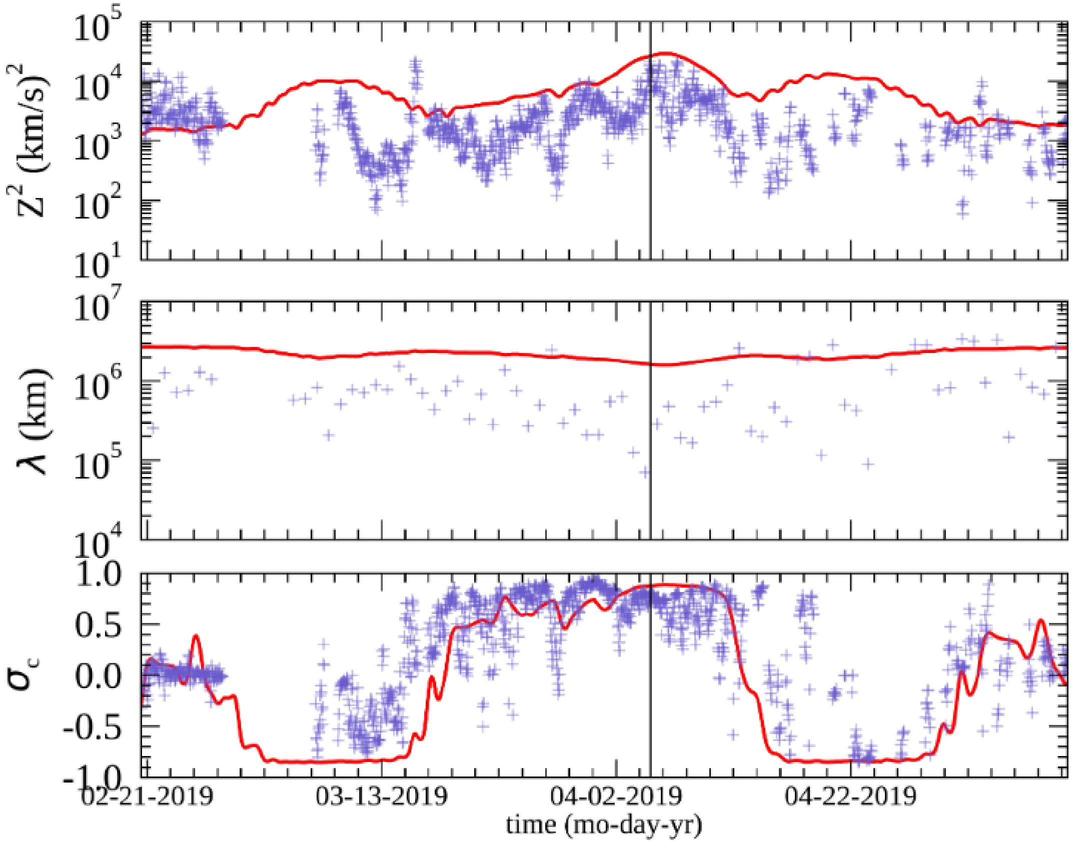

- Comparison of time series for O2. Left: Bulk flow parameters Right: Turbulence parameters.
- Symbols show hourly averages of PSP data; red curves show model results; shaded regions in V_R and B_R panels shows +/- rms turbulence amplitude from model

Comparisons of model with PSP Orbits 1, 3, and 4

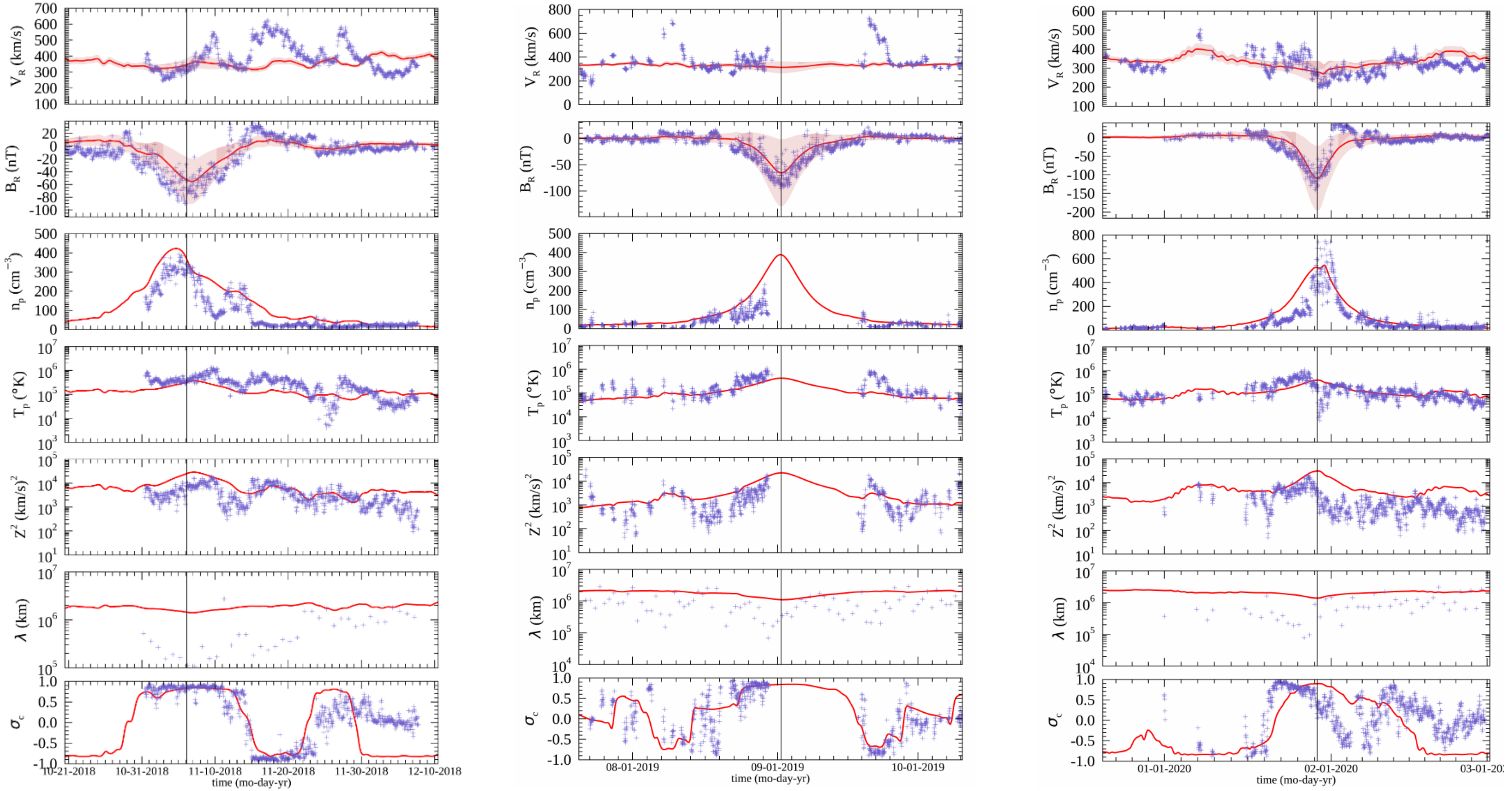

Comparisons of model with PSP Orbit 5

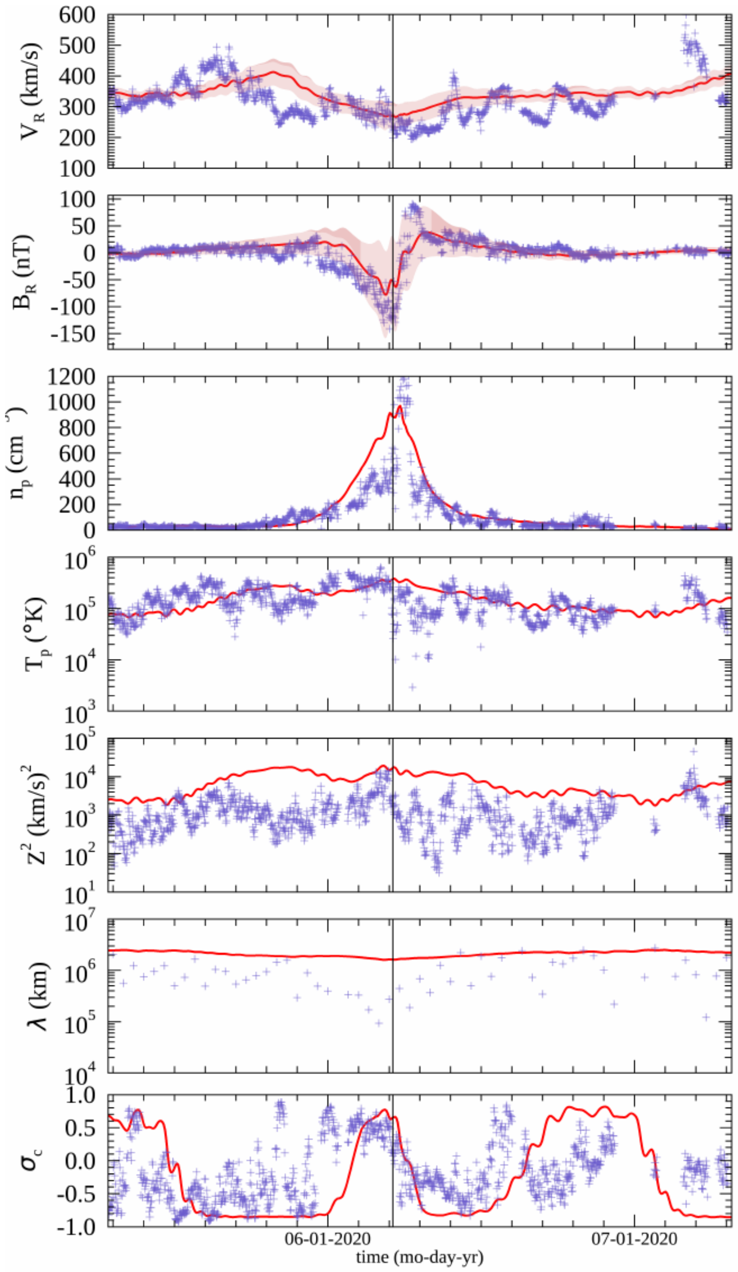

- For all orbits, general agreement between model and observations
- Some transient high-speed streams seen in observations (especially E1) are not captured in the model. Limited resolution of magnetograms at inner boundary?
- Modeled turbulence energy often larger (x 1.5-2) than observations
- Observed correlation scale at PSP perihelia several times smaller than model result
- Some heliospheric current sheet crossings are captured (inferred from reversal of cross helicity)

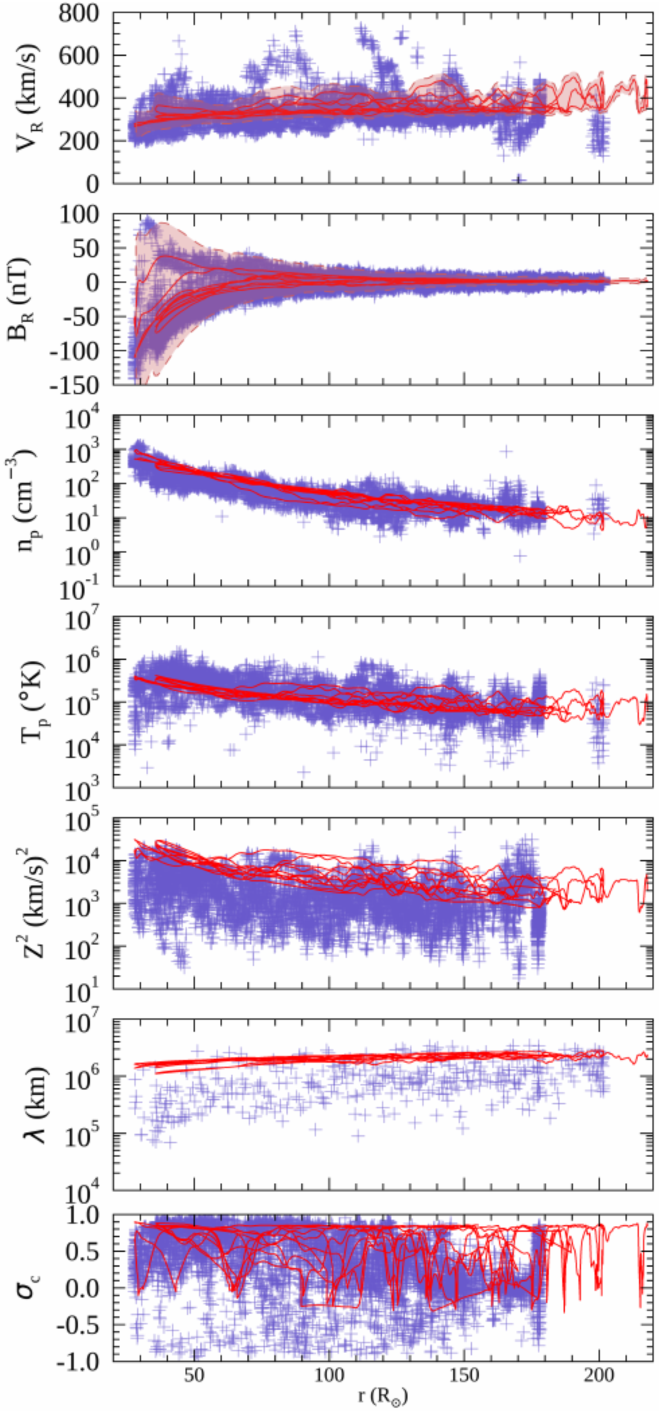

Radial trends aggregrated from first five PSP orbits

- Left: PSP data (symbols) aggregated from Orbits 1 to 5. Red curves show results from model, accumulated from five runs corresponding to the five respective orbits.
- ~95% of data are slow wind (<400 km/s)
- Right: Mean values within bins of 10 solar radii from PSP data (blue circles) and model (red diamonds). Bars above and below symbols represent standard deviation.
- Averages reveal that radial trends in mean flow are quite well captured by model (regardless of transient features seen in time series plots)
- Broad trends in turbulence properties also reproduced

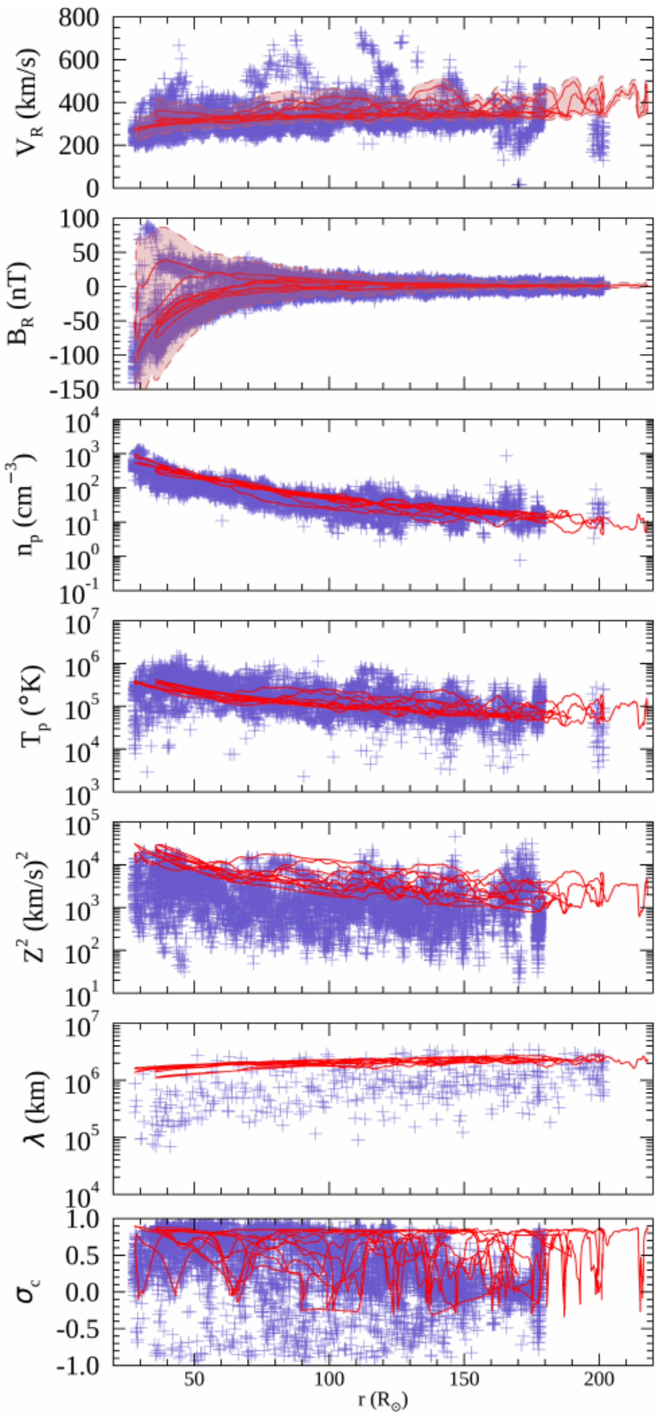

Radial trends aggregrated from first five PSP orbits

- Left: PSP data (symbols) aggregated from Orbits 1 to 5. Red curves show results from model, accumulated from five runs corresponding to the five respective orbits.
- ~95% of data are slow wind (<400 km/s)
- Right: Mean values within bins of 10 solar radii from PSP data (blue circles) and model (red diamonds). Bars above and below symbols represent standard deviation.
- Averages reveal that radial trends in mean flow are quite well captured by model (regardless of transient features seen in time series plots)
- Broad trends in turbulence properties also reproduced

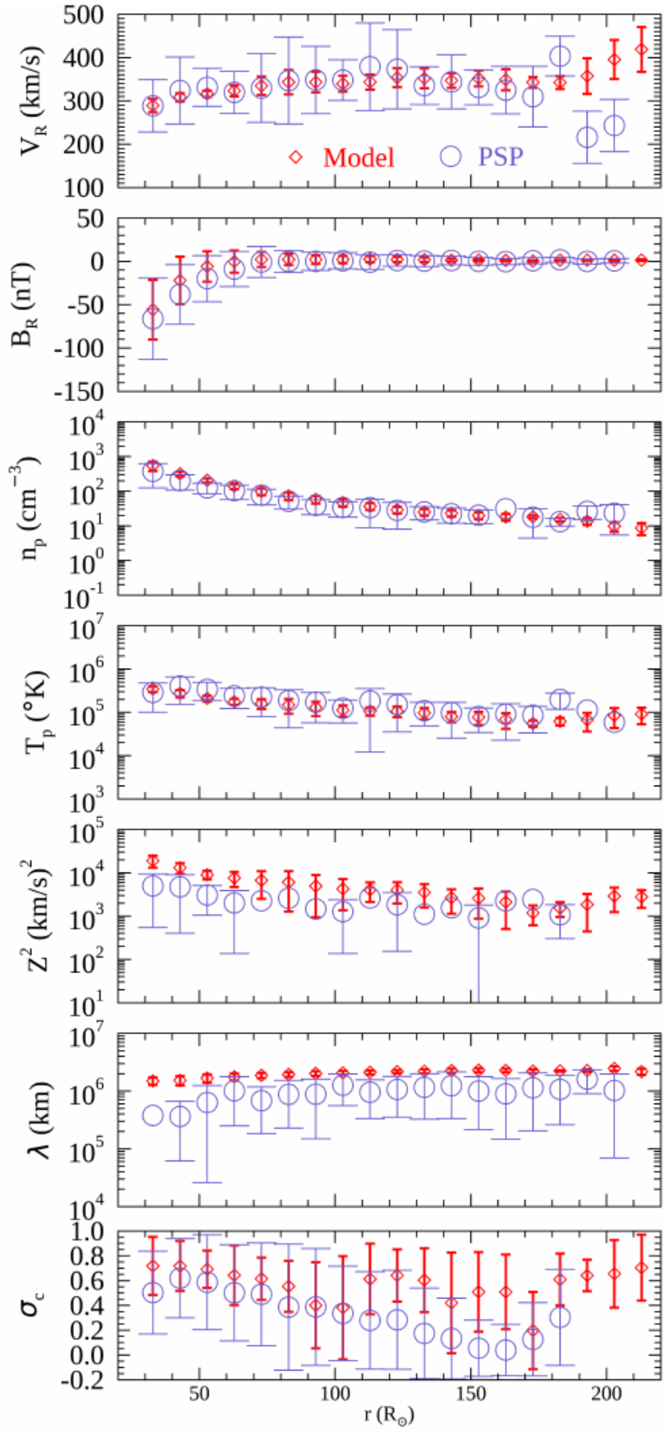

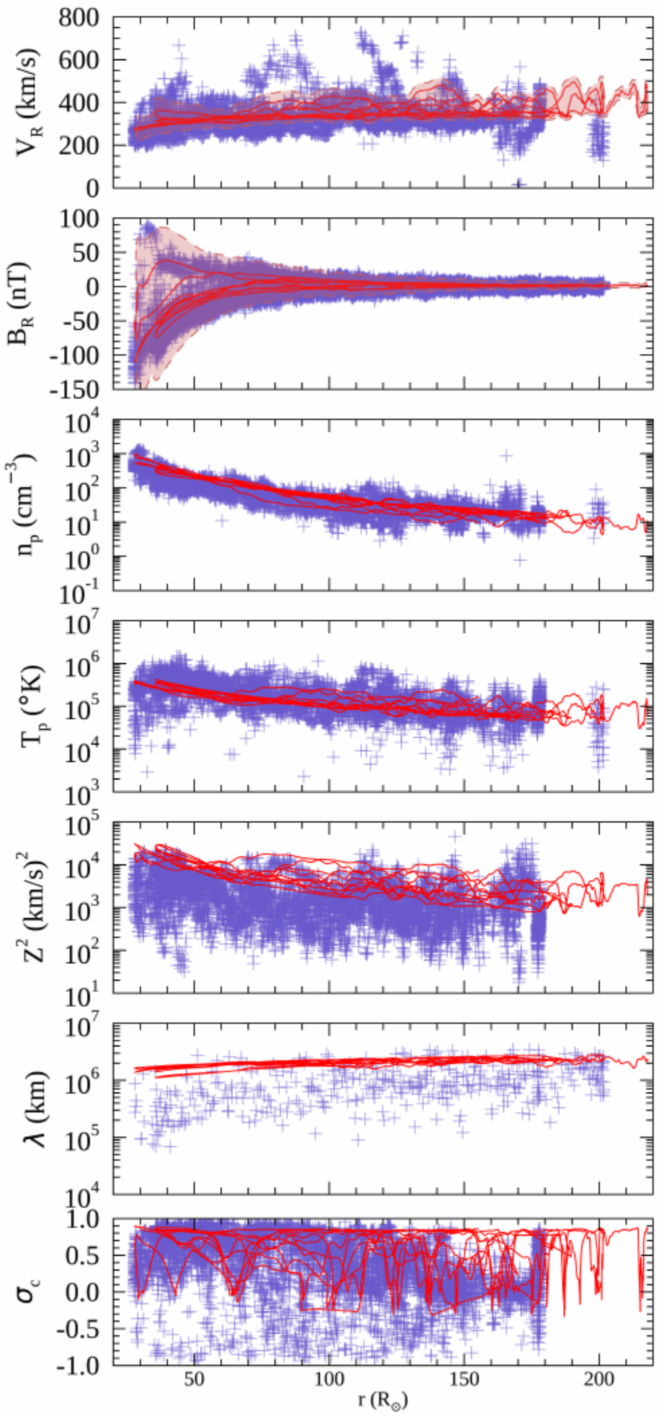

Radial trends aggregrated from first five PSP orbits

Power-law fits to heliocentric distance:

$X \propto r^\gamma$	γ
V_R	0.012 ± 0.007
B_R	-2.036 ± 0.020
B_T	-1.172 ± 0.023
n_p	-1.685 ± 0.015
T_p	-0.813 ± 0.019
Z^2	-0.713 ± 0.031
λ	0.746 ± 0.074

- *Helios* (0.2-1 AU): $T_p \propto r^{-.9}$ (Perrone+ 2019)
- 1+ AU: $T_p \propto r^{-.5}$ (Richardson+ 1995)
- Heating weaker in young solar wind?
- Small λ near perihelia could be due to PSP sampling variations parallel to mean $\boldsymbol{B}$ ("slab" turbulence)

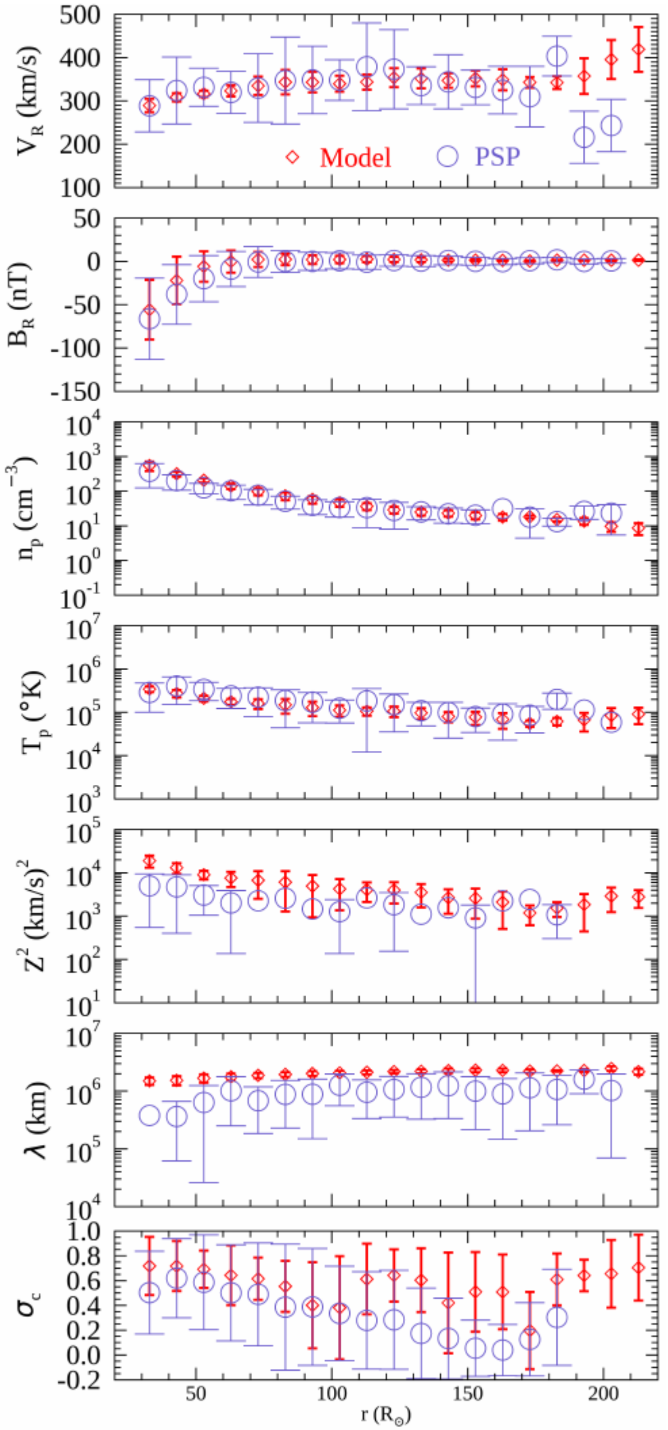

Summary

- Two-fluid MHD model, with resolved mean-flow and “subgrid-scale” turbulence
- Model is being compared with near-Sun data for the first time with PSP
- General agreement between model and data; radial trends well captured, esp. bulk flow
- Turbulence measured by PSP near Sun may be biased by sampling parallel to mean $\boldsymbol{B}$
- Planned improvements –
  - Higher-res B.C.s
  - Inclusion of transition region (currently model starts at coronal base)

More details – Chhiber+ 2021, ApJ (in press; https://arxiv.org/abs/2107.11657)

Extra Slides

Radial Trend in Correlation Scale

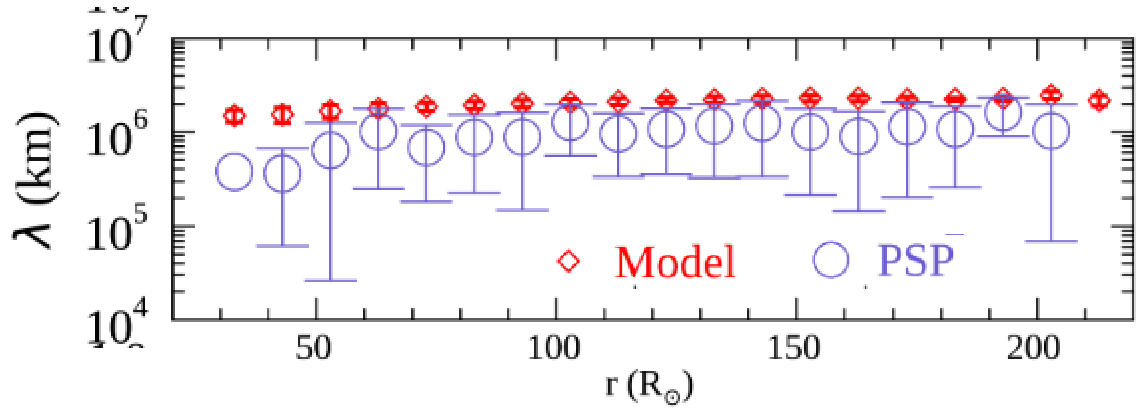

λ near PSP perihelia is smaller than expected from model, and from radial trend obtained from 1+ AU measurements

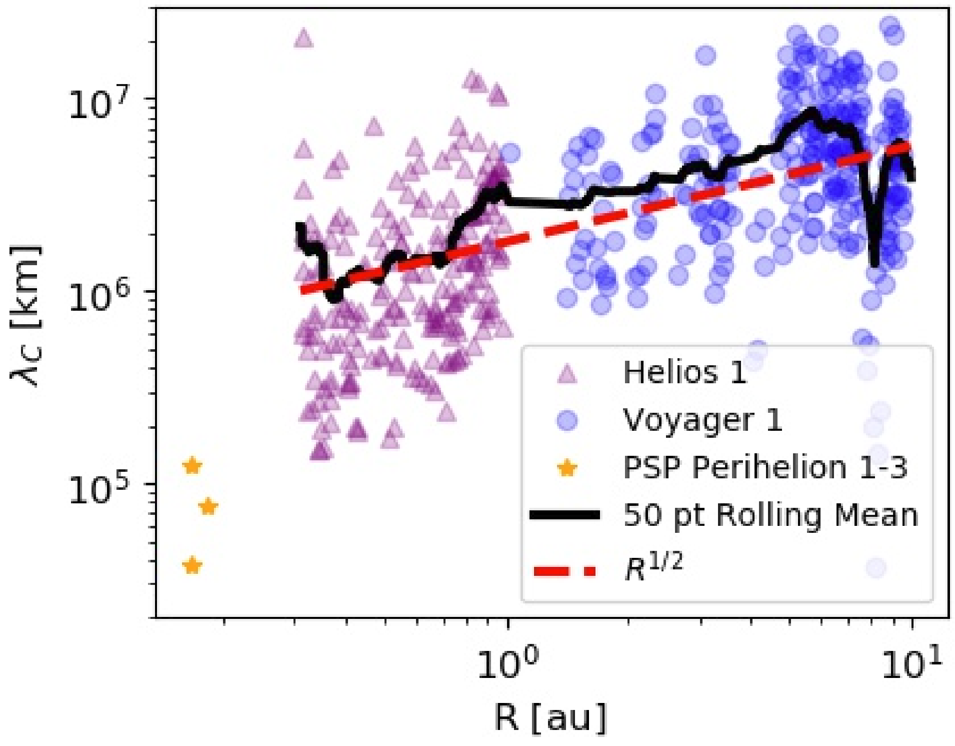

Cuesta+ (submitted)

Fraction of PSP data with flow quasi-aligned with magnetic field

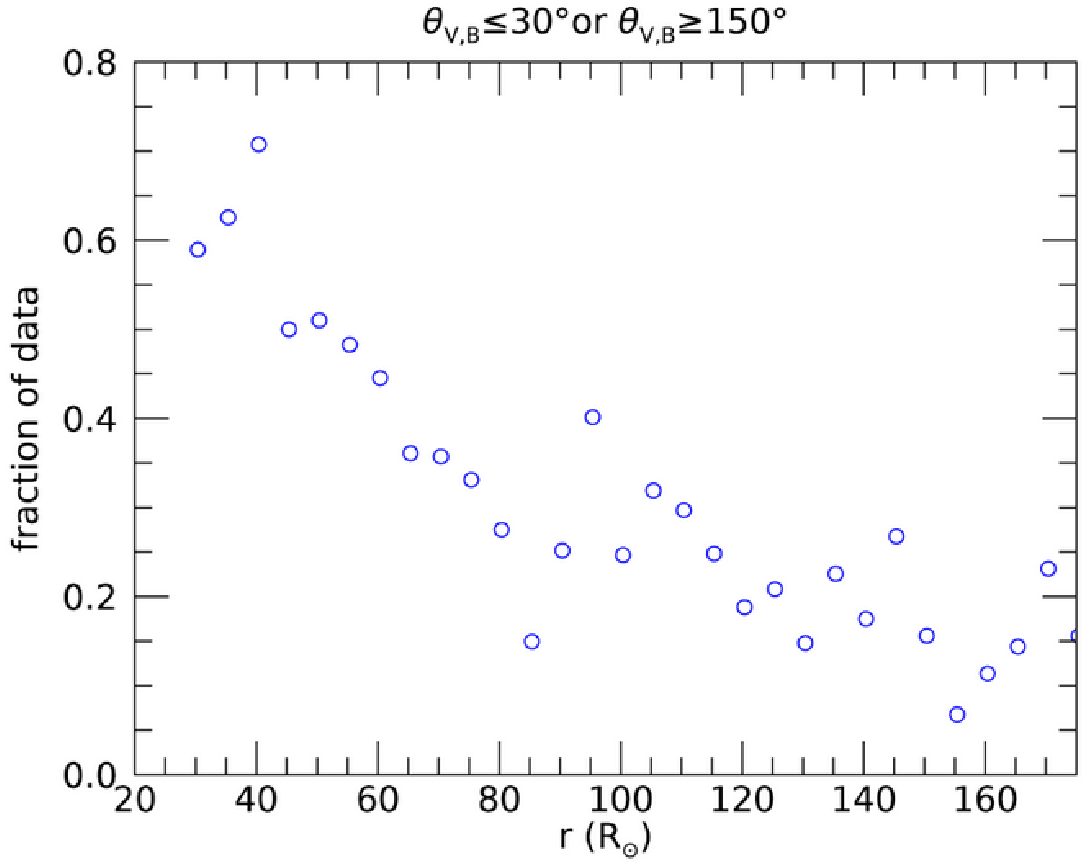

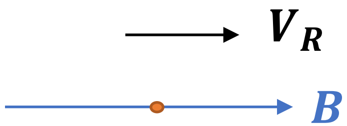

PSP perihelia

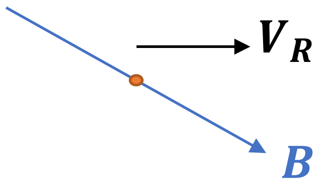

Near Earth

PSP mainly sampling variations parallel to $\boldsymbol{B}_0$ near Sun

Radial Trend in Correlation Scale

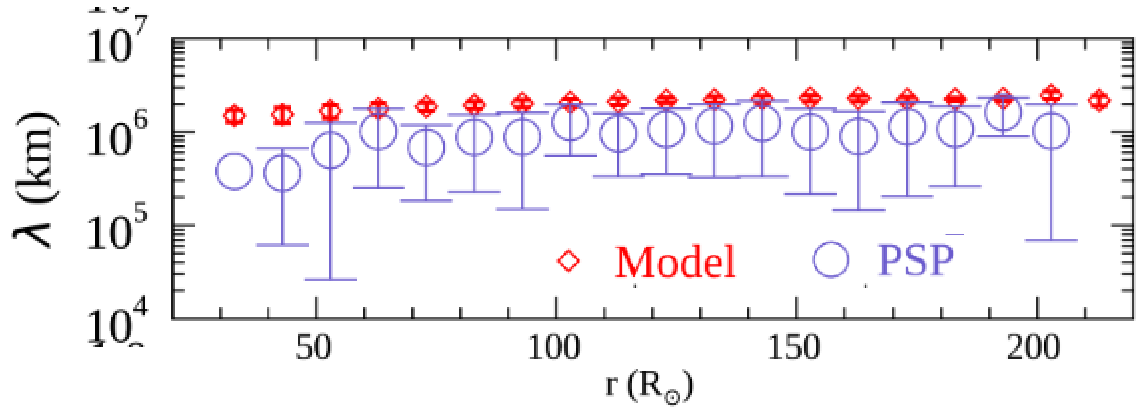

- PSP sampling variations parallel to $\boldsymbol{B}_0$ ("slab" turbulence) near Sun, which appear to have smaller correlation scale (Ruiz+ 2011; Adhikari+ 2020)

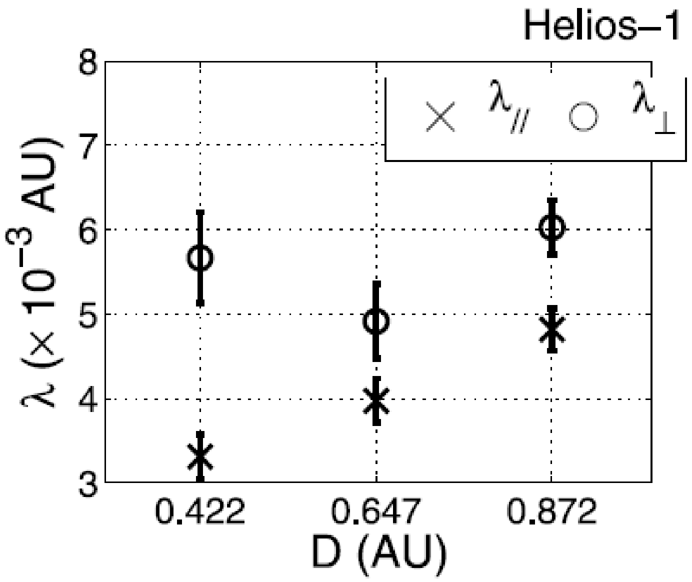

Ruiz+ 2011

Two-fluid MHD Solar Wind Model

(in frame corotating with Sun):

- Continuity eqn. – $$\frac{\partial\tilde{\rho}}{\partial t} + \nabla\cdot(\tilde{\rho}\tilde{\mathbf{v}}) = 0$$
- Momentum eqn. – $$\frac{\partial\tilde{\mathbf{v}}}{\partial t} + (\tilde{\mathbf{v}}\cdot\nabla)\tilde{\mathbf{v}} + \frac{1}{\tilde{\rho}}\nabla(\tilde{P}_S + \tilde{P}_E) - \frac{(\nabla\times\tilde{\mathbf{B}})\times\tilde{\mathbf{B}}}{4\pi\tilde{\rho}} + \frac{GM_\odot}{r^2}\hat{\mathbf{r}} + 2\boldsymbol{\Omega}\times\tilde{\mathbf{v}} + \boldsymbol{\Omega}\times(\boldsymbol{\Omega}\times\mathbf{r}) = 0$$
- Induction eqn. – $$\frac{\partial\tilde{\mathbf{B}}}{\partial t} = \nabla\times(\tilde{\mathbf{v}}\times\tilde{\mathbf{B}})$$
- Energy eqn. for protons – $$\frac{\partial\tilde{P}_S}{\partial t} + (\tilde{\mathbf{v}}\cdot\nabla)\tilde{P}_S + \gamma\tilde{P}_S\nabla\cdot\tilde{\mathbf{v}} = (\gamma-1)\left(\frac{\tilde{P}_E - \tilde{P}_S}{\tau_{SE}} + f_p Q_T\right)$$
- Energy eqn. for electrons – $$\frac{\partial\tilde{P}_E}{\partial t} + (\tilde{\mathbf{v}}\cdot\nabla)\tilde{P}_E + \gamma\tilde{P}_E\nabla\cdot\tilde{\mathbf{v}} = (\gamma-1)\left[\frac{\tilde{P}_S - \tilde{P}_E}{\tau_{SE}} - \nabla\cdot\mathbf{q}_E + (1-f_p)Q_T\right]$$

Two-Fluid Reynolds Averaged MHD Equations

$$\widetilde{\boldsymbol{B}} = \boldsymbol{B} + \boldsymbol{B}'$$
$$\widetilde{\boldsymbol{u}} = \boldsymbol{u} + \boldsymbol{u}'$$

$$\frac{\partial \rho}{\partial t} + \nabla \cdot (\rho \mathbf{v}) = 0$$

$$\frac{\partial (\rho \mathbf{u})}{\partial t} + \nabla \cdot \left[\rho \mathbf{v}\mathbf{u} - \frac{1}{4\pi}\mathbf{B}\mathbf{B} + \left(P_S + P_E + \frac{B^2}{8\pi} + \frac{\langle B'^2 \rangle}{8\pi} \right) \mathbf{I} + \boldsymbol{\mathcal{R}} \right] = -\rho \left(\frac{G M_\odot}{r^2} + \boldsymbol{\Omega} \times \mathbf{u} \right)$$

$$\frac{\partial \mathbf{B}}{\partial t} = \nabla \times (\mathbf{v} \times \mathbf{B} + \boldsymbol{\varepsilon}_m \sqrt{4\pi\rho})$$

$$\frac{\partial P_S}{\partial t} + (\mathbf{v} \cdot \nabla) P_S + \gamma P_S \nabla \cdot \mathbf{u} + (\gamma - 1) \frac{P_S - P_E}{\tau_{SE}} = f_p Q_T$$

$$\frac{\partial P_E}{\partial t} + (\mathbf{v} \cdot \nabla) P_E + \gamma P_E \nabla \cdot \mathbf{u} + (\gamma - 1) \left[\frac{P_E - P_S}{\tau_{SE}} + \nabla \cdot \mathbf{q}_H \right] = (1 - f_p) Q_T$$

- P_S and P_E are the proton and electron pressure
- $\mathbf{u}$ is the velocity in the inertial frame
- $\mathbf{v}$ is the velocity in the rotating frame
- τ_{SE} is the electron-proton Coulomb collision rate
- $\boldsymbol{\mathcal{R}} = \langle \rho \mathbf{v}'\mathbf{v}' - \frac{\mathbf{B}'\mathbf{B}'}{4\pi} \rangle$ is the Reynolds stress tensor
- $\boldsymbol{\varepsilon}_m = \frac{\langle \mathbf{v}' \times \mathbf{B}' \rangle}{(4\pi\rho)^{1/2}}$ is the mean turbulent electric field
- Q_T is the turbulent heating rate
- $\mathbf{q}_H$ is the electron heat flux

Closures and other terms (extra slide)

- Electron-proton collision frequency:

$$\nu_E = \frac{8(2\pi m_e)^{1/2} e^4 N_E \ln\Lambda}{3m_p(k_B T_E)^{3/2}} \qquad \ln\Lambda = \ln\left[\frac{3(k_B T_E)^{3/2}}{2\pi^{1/2} e^3 N_E^{1/2}}\right]$$

- Classical (Spitzer) electron heat conduction (below 5 $R_\odot$):

$$\mathbf{q}_\mathrm{S} = -\kappa\hat{\mathbf{B}}(\hat{\mathbf{B}}\cdot\nabla)T_E \qquad \kappa = 8.4\times 10^{-7}\,T_E^{5/2}$$

- Collisionless (Hollweg) heat conduction: $\mathbf{q}_\mathrm{H} = (3/2)\alpha_\mathrm{H} P_E \mathbf{v}$

- Turbulent heating: $Q_T = \dfrac{\alpha f^+(\sigma_c)\rho Z^3}{2\lambda}$
- TSDIA closure for turbulent stresses:

$$\boldsymbol{\varepsilon}_m = \bar{\alpha}\mathbf{B} - \bar{\beta}\nabla\times\mathbf{V}_A + \bar{\gamma}\nabla\times\mathbf{v}$$

$$\nu_M = (7/5)\bar{\gamma}$$

$$\nu_K = (7/5)\bar{\beta}$$

$$\frac{1}{\rho}\boldsymbol{\mathcal{R}} = \frac{2}{3}K_R\,\mathbf{I} - \nu_K\boldsymbol{\mathcal{S}} + \nu_M\boldsymbol{\mathcal{M}}$$

$$K_R = \sigma_D Z^2/2$$

$$\boldsymbol{\mathcal{S}} = \nabla\mathbf{u} + \nabla\mathbf{u}^T - \frac{2}{3}(\nabla\cdot\mathbf{u})\mathbf{I}$$

$$\boldsymbol{\mathcal{M}} = \nabla\mathbf{V}_A + \nabla\mathbf{V}_A^T - \frac{2}{3}(\nabla\cdot\mathbf{V}_A)\mathbf{I}$$

$$\nu_K \approx 0.27 Z\lambda \qquad \nu_M \approx 0.22\sigma_c Z\lambda$$

Modeling NL terms

$$\frac{\partial\mathbf{z}_\pm}{\partial t} = -\mathbf{z}_\mp\cdot\nabla\mathbf{z}_\pm$$

$$\frac{\partial}{\partial t}\langle z_+^2\rangle = -2\langle\mathbf{z}_+\cdot(\mathbf{z}_-\cdot\nabla\mathbf{z}_+)\rangle$$

$$\sim -\langle z_+^2\rangle\frac{\langle z_-^2\rangle^{-1/2}}{\lambda_+},$$

$$\frac{\partial Z^2}{\partial t} \sim -\frac{Z^3}{\lambda}$$

Usmanov et al., 2018

Boundary/Initial conditions and parameters (extra slide)

Symbol	Description	Value
N_0	proton number density in the initial state at 1 $R_\odot$	$8 \times 10^7\,\mathrm{cm}^{-3}$
T_0	electron and proton temperature in the initial state at 1 $R_\odot$	$1.8 \times 10^6\,\mathrm{K}$
B_0	magnetic field strength of dipole at 1 $R_\odot$	12 G
δv_0	driving amplitude of fluctuations in the initial state at 1 $R_\odot$	$35\,\mathrm{km\,s^{-1}}$
σ_{c0}	normalized cross helicity in the initial state	0.8
λ_0	correlation scale of turbulence in the initial state at at 1 $R_\odot$	0.015 $R_\odot$

Symbol	Description	Value
σ_D	normalized energy difference (residual energy)	$-1/3$
γ	adiabatic index	$5/3$
α_{H}	constant in Hollweg's collisionless heat flux	1.05
α, β	Kármán–Taylor constants	2, 0.128
f_p	fraction of turbulent heating for protons	0.6
r_{H}	collisional/collisionless electron heat flux transition region	5 $R_\odot$

Usmanov et al., 2018

Spatial Scales Resolved in Simulations

- Resolution ~ $700 \times 120 \times 240$ in r, θ, ϕ ($r = 1\ R_{\odot}$ - 5 AU)
- Grid scale Δ is generally within a factor of few correlation scales

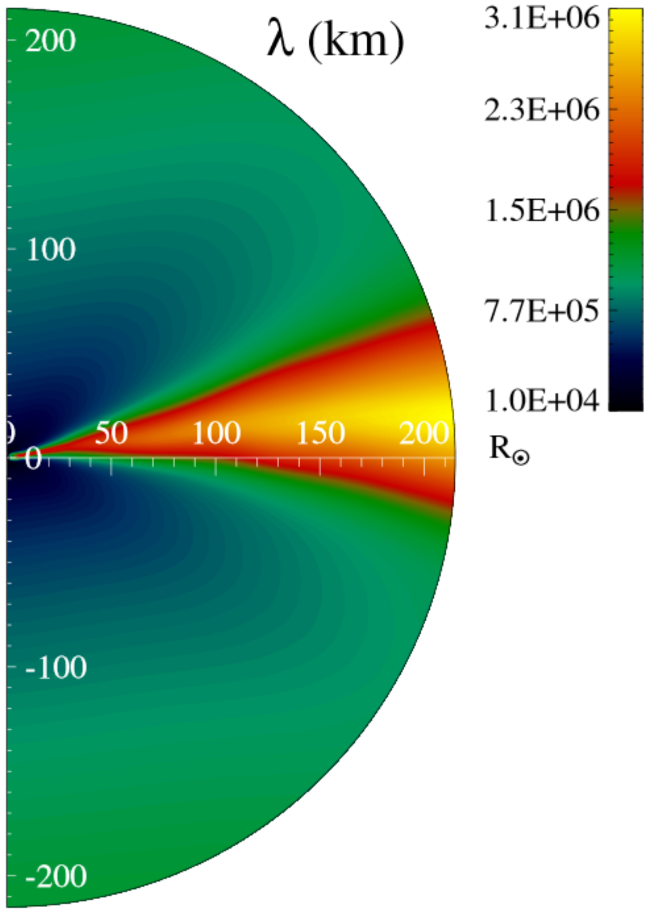

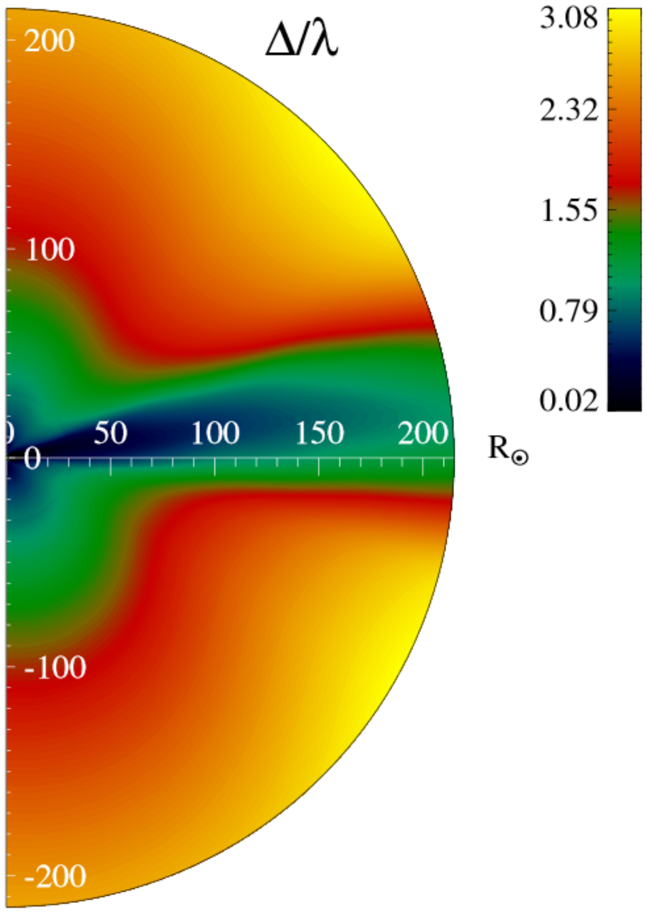

Sample Results – Meridonal planes (30 Rs to 5 AU) and Comparison with Ulysses Data

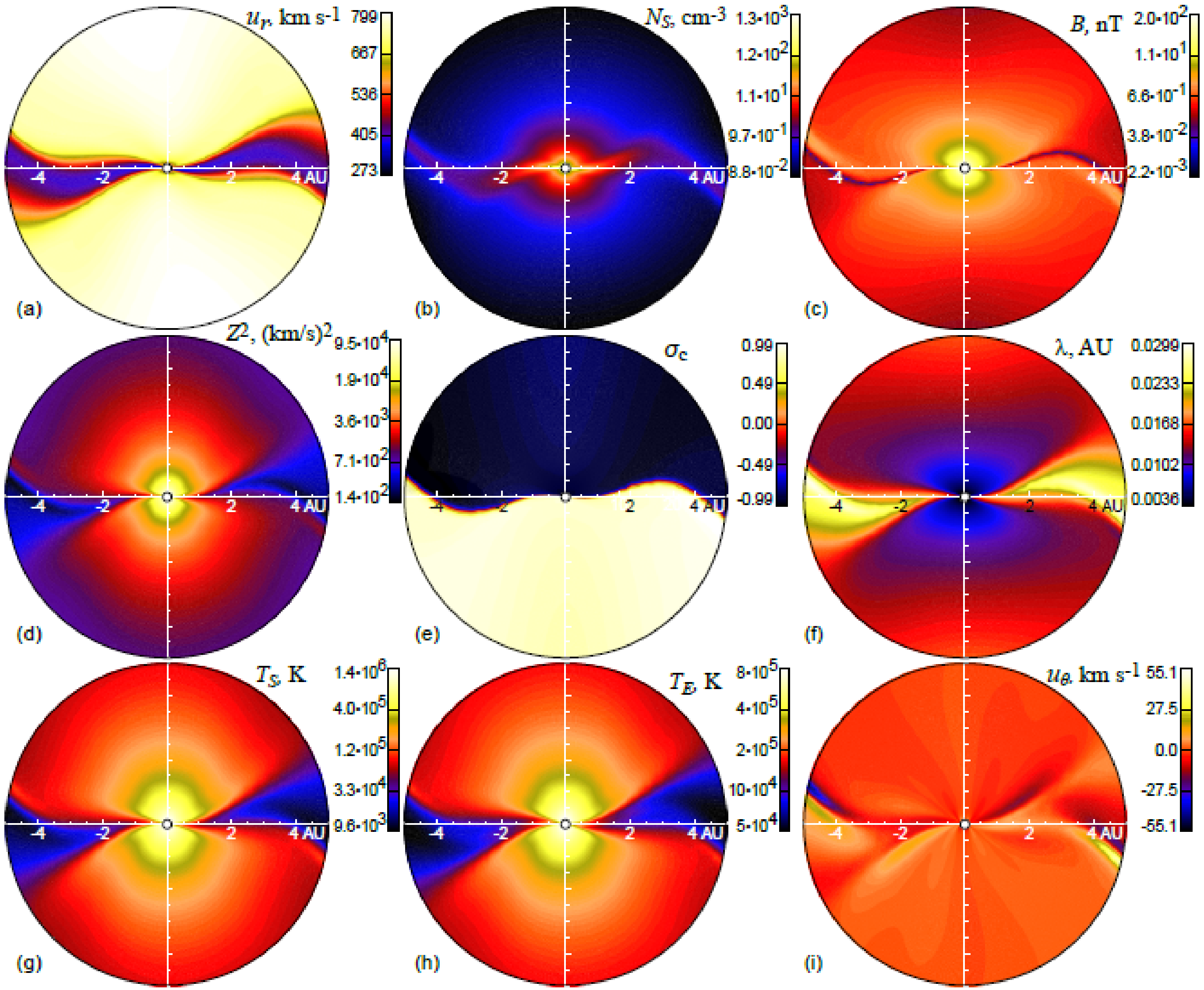

Usmanov et al., 2018

Comparison with Ulysses observations from 1994-1995

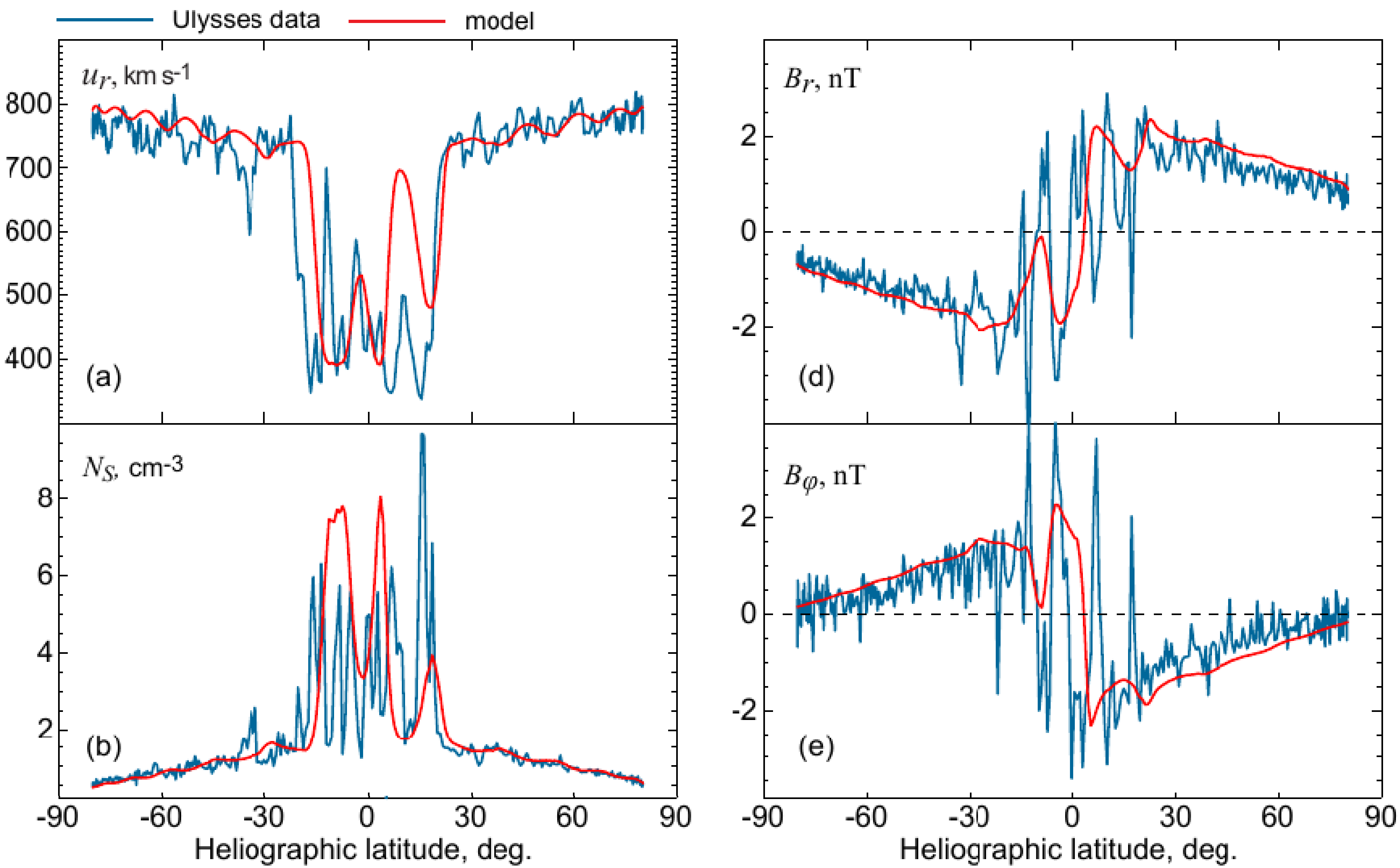

Usmanov et al., 2018

Radial Trend in Correlation Scale - slab and 2D turbulence

$$\mathbf{b}(x,y,z) = \mathbf{b}_{\mathrm{2D}}(x,y) + \mathbf{b}_{\mathrm{slab}}(z)$$

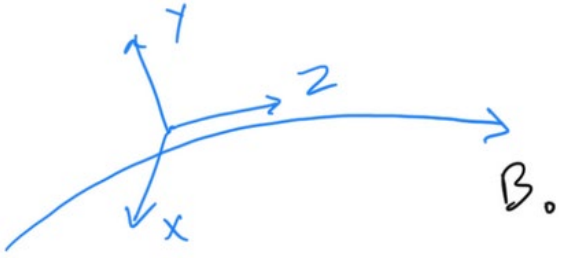

- B_0 introduces anisotropy in MHD turbulence
- Slab component – Alfven waves propagating along B_0
- 2D component – strong turbulence from perpendicular cascade
- Slab/2D energy ratio is ~20/80, near Earth
- Will PSP be able to measure turbulent variations perpendicular to B_0 close to Sun?

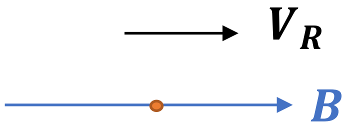

PSP perihelia

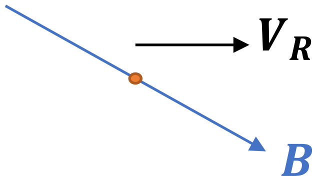

Near Earth

Issues - Model gives large cross helicity near 1 AU

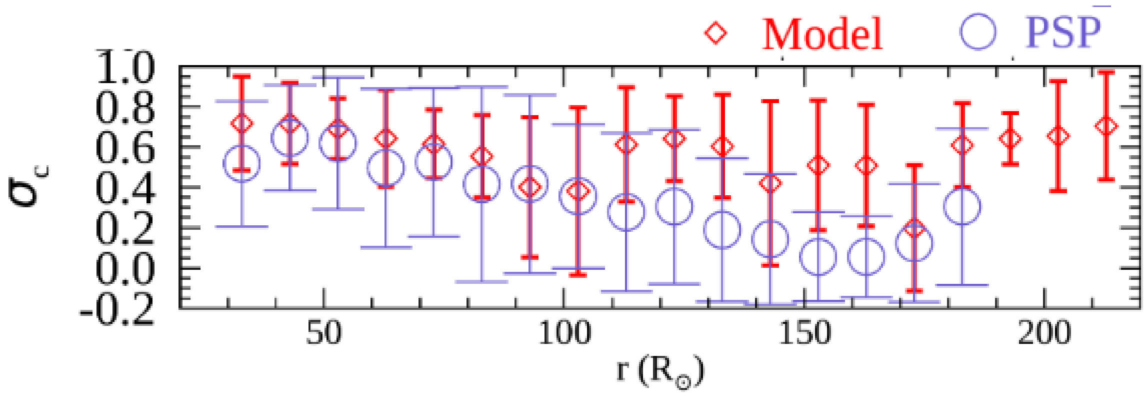

- Shear can reduce σ_c
- Model missing shear? Coarse resolution may not be capturing ΔU and ΔB
- Some models use phenomenological shear driving terms (Zank+ 1996, Breech+ 2008, Adhikari+ 2017)
- Shear term in evolution equation for turbulence energy: $\sim \frac{\Delta U_i}{\Delta x_j} \sim C_{\mathrm{sh}} \frac{U}{r}$
- $C_{\mathrm{sh}} = \frac{\Delta U}{U}$